Treating a 0.22 g of **4** with 0.39 mL of aqueous formaldehyde and 0.48 mL of piperidine for 24 h as described for **3a**, 0.25 g (75.8%) of **5b** was obtained. mp 172 ℃ dec. ^{1}H NMR (DMSO-d_6) δ 6.90-6.52 (m, 12H, ArH), 5.79 (m, 2H, -CH=), 5.00-4.88 (m, 4H, $=CH_2$), 4.11 (br s, 4H, $-CH_2C=$), 3.53 (br s, 12H, $ArCH_2Ar$), 3.09 (br s, 8H, $ArCH_2N$-), 2.62 (br s, 16H, $-NCH_2$-), 1.50 and 1.38 (two br s, 24H, $-CH_2$-).

References

1. Gutsche, C. D. *Topics in Current Chemistry* **1984**, *123*, Springer, Berlin, Heidelberg.
2. (a) Gutsche, C. D.; Alam, I. *Tetrahedron* **1988**, *44*, 4689. (b) Gutsche, C. D.; Alam, I. *J. Org. Chem* **1990**, *55*, 4487. (c) Shinkai, S.; Mori, S.; Tsubaki, T.; Sone, T.; Manabe, O. *Tet. Lett.* **1984**, *25*, 5315.
3. Atwood, J. L.; Koutsantonis, G. A.; Raston, C. L. *Nature* **1994**, *368*, 229.
4. (a) Shinkai, S.; Koreishi, H.; Ueda, K.; Arimura, T.; Manabe, O. *J. Am. Chem. Soc.* **1987**, *109*, 6371. (b) Shinkai, S.; Otsuka, T.; Araki, K.; Matsuda, T. *Bull. Chem. Soc. Jpn.* **1989**, *62*, 4055. (c) Chang, S. K.; Cho, I. *Chem. Lett.* **1984**, 477. (d) Nomura, E.; Taniguchi, H.; Tamura, S. *Chem. Lett.* **1989**, 1125.
5. (a) Kanamathareddy, S.; Gutsche, C. D. *J. Am. Chem. Soc.* **1993**, *115*, 6572. (b) Rogers, J. S.; Gutsche, C. D. *J. Org. Chem.* **1992**, *57*, 3152. (c) Kanamathareddy, S.; Gutsche, C. D. *J. Org. Chem.* **1992**, *57*, 3160.
6. Casnati, A.; Minari, P.; Pochini, A.; Ungaro, R. *J. Chem. Soc., Chem. Commun.* **1991**, 1413.
7. Otsuka, H.; Araki, K.; Shinkai, S. *J. Org. Chem.* **1994**, *59*, 1542.
8. Gutsche, C. D.; Nam, K. C. *J. Am. Chem. Soc.* **1988**, *110*, 6153.
9. Gutsche, C. D.; Levin, J. A.; Sujeeth, P. K. *J. Org. Chem.* **1985**, *50*, 5802.
10. Gutsche, C. D.; Iqbal, M. *Org. Syn.* **1990**, *68*, 234.
11. Gutsche, C. D.; Lin, L. G. *Tetrahedron* **1986**, *42*, 1633.
12. Neri, P.; Pappalardo, S. *J. Org. Chem.* **1993**, *58*, 1048.
13. Nam, K. C.; Yoon, T. H. *Bull. Kor. Chem. Soc.* **1993**, *14*, 169.

The Adsorption and Decomposition of NO on a Stepped Pt(111) Surface

S. B. Lee*, D. H. Kang, C. Y. Park†, and H. T. Kwak‡

Department of Chemistry, Sung Kyun Kwan University, Suwon 440-746, Korea
†Department of Physics, Sung Kyun Kwan University, Suwon 440-746, Korea
‡Department of Chemistry, Kook Min University, Seoul 136-701, Korea
Received December 8, 1994

The adsorption and decomposition of NO on a stepped Pt(111) surface have been studied using thermal desorption spectroscopy and Auger electron spectroscopy. NO adsorbs molecularly in two different states of the terrace and the step, which are distinguishable in thermal desorption spectra. NO dissociates *via* a bent species at the step sites on the basis of vibrational spectrum data reported previously. The dissociation of NO is an activation process : the activation energy is estimated to be about 2 kcal/mol. Increase in the NO dissociation with adsorption temperature is explained by a process controlled by diffusion of the dissociated atomic nitrogen from the step to the terrace of the surface. In addition to NO and N_2, the desorption peak of N_2O is observed. We conclude that the formation of N_2O is attributed to surface reaction of NO and N adsorbed on the surface.

Introduction

The adsorption and reaction of nitric oxide on metal surface are interesting in both fundamental and technological aspects.[1] The catalytic reduction of nitric oxide plays an important role in control of air pollution. NO and CO are two of the most widely studied adsorbates because of its simplicity. They have similar electronic structures except that NO has an unpaired electron in the antibonding 2π orbital. This causes more complex behaviors in chemisorption and reaction of NO than those of CO. CO adsorbs only molecularly on noble metals. In contrast, as for NO on noble metals there are evidences for dissociative adsorption at low temperatures as well as molecular adsorption with various geometries, including tilt, bent, and linear NO at two-fold and on-top sites.[2-16]

Gorte *et al.*[7] reported that the desorption spectra of NO adsorbed on Pt(111), (110) and (100) show different shapes and different peak temperatures. In their report, the desorption activation energies for major tightly-bound states on the (100), (110) and (111) planes are 36, 33.5 and 25 kcal/mol, respectively, and the fraction of the dissociation is less than 2% on Pt(111) surface. Ertl *et al.*[9] also studied the interaction of NO with Pt(111) surface using molecular beam technique and thermal desorption spectroscopy (TDS), and reported

We dedicate this work to Professor Woon-Sun Ahn on the occasion of his retirement.

that the molecular adsorption predominates. They reported the NO dissociation is restricted to defect sites and the activation energy and the pre-exponential factor for the desorption are 33.1 kcal/mol and $10^{15.5}$/sec, respectively.

In a more recent study, Agrawal and Trenary[16] have used an infrared reflection-absorption spectroscopy (IRAS) to characterize NO at the defect sites. The adsorbed molecules at the defect sites show IR bands in the range of 1820-1840 cm^{-1}, a characteristic of linear Pt-N-O configuration, while bent Pt-N-O configuration has the bands around 1609-1634 cm^{-1}. Other IR bands are assigned to NO at the terminal sites (1700-1720 cm^{-1}) and the two-fold bridge sites (1475-1500 cm^{-1}) of the (111) terrace.

In our previous study for the decomposition of NO on an Ar-ion sputtered Pt(111) surface,[17] effects of the defect sites on the decomposition have been investigated. The thermal desorption spectra obtained for the uniform Pt(111) saturated with NO at 300 K indicate that the chemisorption of nitric oxide is predominantly molecular. The Ar-ion sputtering, on the other hand, produces more strongly bound β-state, through which the dissociation of NO is promoted. On the basis of vibrational spectroscopic data reported previously,[16] NO at the defect sites was characterized by two types of structures, terminal linear and bent. And it was also argued that the bent species contributes to the dissociation of NO.

In this paper, we report kinetics of the decomposition of NO and the production of N_2O from the decomposed species on a stepped Pt(111) surface. The stepped sites is expected play similar roles to the defect sites. But we anticipate more quantitative analysis can be carried out with the stepped surface.

Experimental

The experiments were carried out in a stainless-steel ultra-high vacuum (UHV) system with the base pressure of 3×10^{-10} torr. The UHV chamber is equipped with a quadrupole mass spectrometer (VG : 200 amu) and a 4-Grid LEED optics for low energy electron diffraction (LEED) and a hemispherical energy analyzer for AES, UPS and XPS. Additional features are an argon ion gun for surface cleaning, an ionization gauge for measuring pressure, and a manipulator for *x*, *y*, *z* motion of the sample. More details of the system are found in previous publications.[17,18]

The stepped platinum single crystal Pt(111) used in the experiments was approximately 8 mm in diameter and 1 mm in thickness. It was prepared by polishing the (111) surface at an angle of about 20° from the (111) orientation and looked like (211) surface on the basis of LEED pattern and TDS, even though it was not correctly identified by Laue method. The crystal was spotwelded onto a pair of W wire (~0.25 mm), which were themselves spotwelded onto a pair of paralled Mo leads (1.5 mm in diameter). These rods were directly connected to a pair of Cu blocks, which were then connected to an electrical feedthrough to heat the crystal resistively. A chromel-alumel thermocouple was spotwelded to the edge of the crystal for temperature measurements.

The stepped Pt(111) crystal was first cleaned using a cycle of Ar-ion bombardment in the range of 300 and 600 K followed by annealing at 1300 K. Then, a short period of ion bombardment or a treatment with low temperature oxygen (1×10^{-7} torr at 700 K for 3 min) followed by brief heating to 1300 K were sufficient to obtain a well-ordered clean surface as identified by LEED and AES.

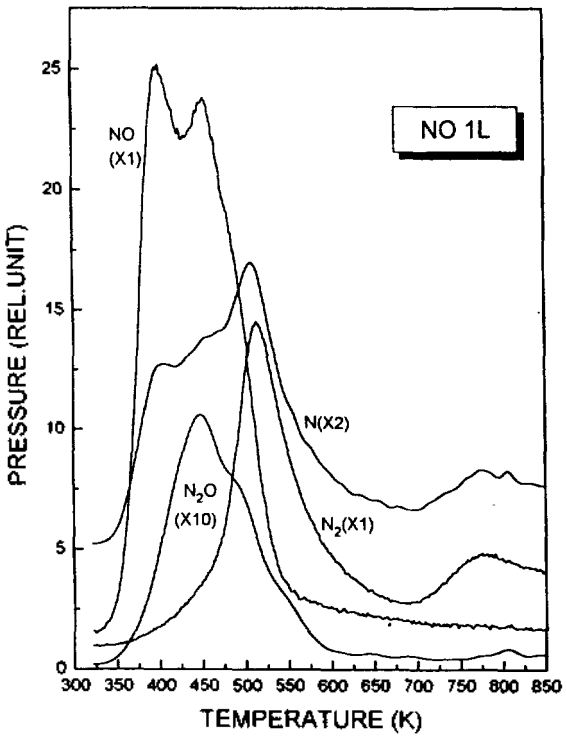

Figure 1. Typical distributions of desorbed species from the stepped Pt(111) surface after NO adsorption of 1 L exposure.

Thermal desorption spectra were obtained by placing the Pt crystal in a line of sight with the mass spectrometer ionizer. The crystal was heated at a rate of about 13.5 K/sec by passing direct current through it. A multiple ion mode in the mass spectrometer was used for simultaneous detection of different species desorbed from the sample. Signals corresponding to C and N were also monitored during the experiments in order to distinguish between N_2 and CO, or N_2O and CO_2.

Results

Figure 1 shows a distribution of desorbed species from the stepped Pt(111) surface after NO adsorption of 1 L exposure at 300 K. It is similar to the desorption spectra obtained from the Ar-ion sputtered Pt(111) surface,[17] except for the peak at mass 44. This peak is an evidence of N_2O formed in a reaction of adsorbed species on the stepped Pt(111) surface, for there is no detectable peak at mass 12 due to the fragments of CO_2 in the corresponding temperature range.

A set of thermal desorption spectra of NO for varying amount of NO exposure are presented in Figure 2. Notice that there are two peaks at 380 and 470 K, which are refered to as α-state and β-state, respectively. As we increase the exposure, the two peaks grow at different rates : the α-state becomes dominant and its peak shifts slightly to a lower temperature at 5 L exposure. The results are similar to the

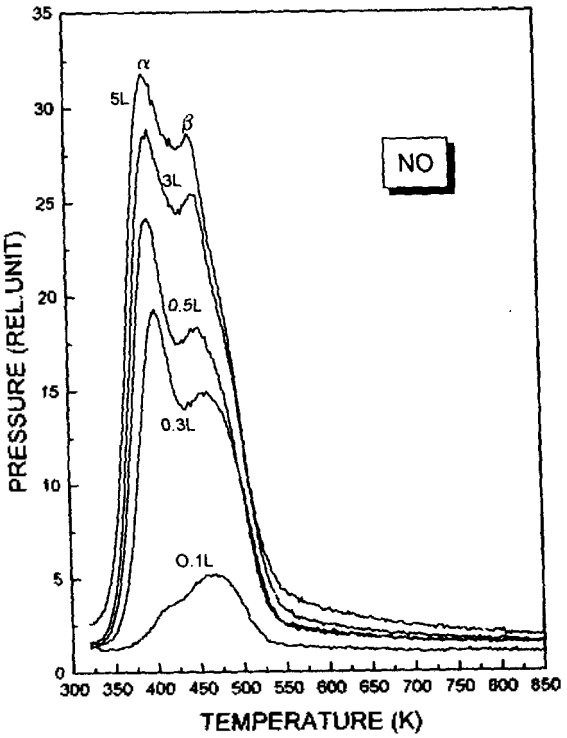

Figure 2. Thermal desorption spectra for NO adsorbed on the stepped Pt(111) with different exposures of NO.

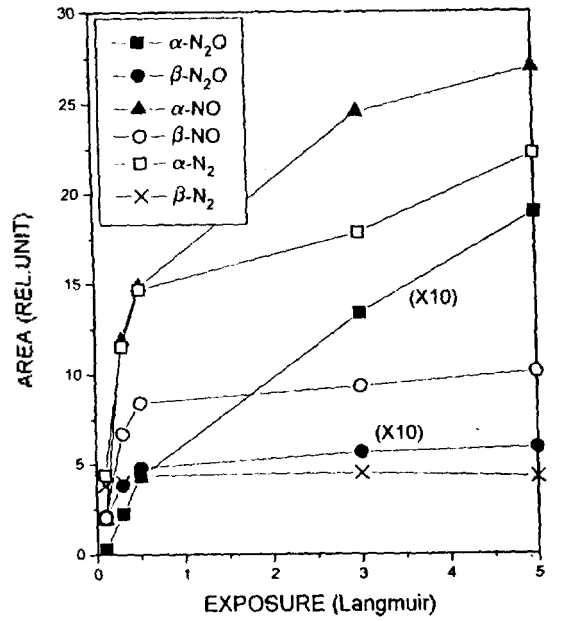

Figure 3. Isotherms for the desorbed species from the stepped Pt(111) at 300 K.

desorption spectra of NO on the Ar-ion sputtered Pt(111) surface[17] or the clean Pt(111) surface.[19] According to previous reports, the α-state comes from the uniform (111) surface and the β-state comes from the stepped sites. Using the method by Redhead,[20] the desorption activation energies for the α-state and the β-state are estimated to be 23 and 28 kcal/mol, respectively.

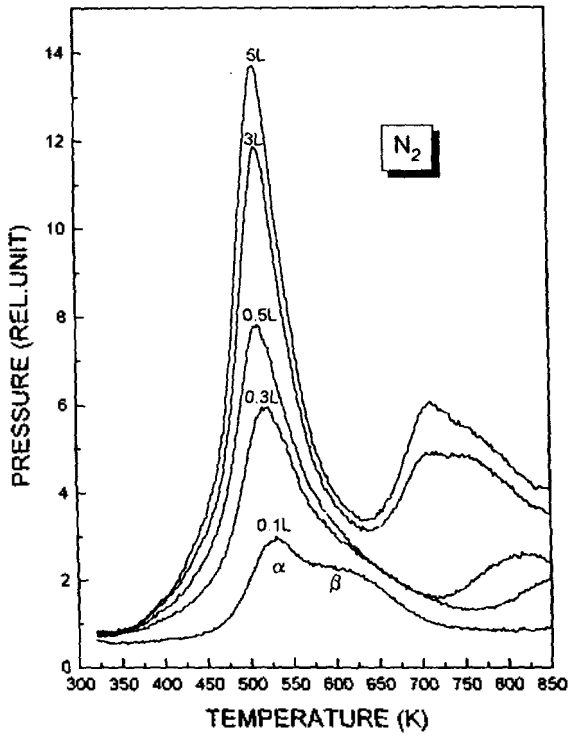

Figure 4. Thermal desorption spectra of N_2 formed from the decomposition of adsorbed NO on the stepped Pt(111) with different exposures of NO.

Using a spectrum deconvolution software, all the desorption spectra are analyzed to estimate the relative amount of desorbed species from each state. In Figure 3 the relative amounts of NO, N_2O and N_2 in the α-state and the β-state are plotted as a function of NO exposure at 300 K. While the amount of the NO desorbed from the α-state increases continuously with increasing exposure, that of the β-state is saturated at the exposure of 0.3 L. At the saturation coverage the β-state is about 30% of total NO population. These results suggest that the stepped surface has a structure similar to Pt(211) surface, which consists of [3(111)×(100)].

Figure 4 shows a set of TDS of N_2 taken simultaneously with TDS of NO (Figure 2). At the exposure of 0.1 L NO, there are two characteristic peaks at 525 and 610 K. The two peaks will also be referred to as α-state and β-state, respectively. In addition to these two peaks a broad peak is observed above 700 K. But we neglect this peak because it is considered as a satellite from the sample supporters such as Mo rods and Cu blocks. Also in order to distinguish the two peaks of N_2 from that of CO, a possible contaminant from the residual gases in UHV chamber, we recorded the mass signals at 12 amu and 14 amu for the fragments of CO and N_2, respectively. But no signals for CO were detected in the range of the desorption temperatures of N_2 and the spectral trace at 14 amu was simply a sum of N_2 and NO traces. We are convinced that the two peaks are for the desorption of N_2. The temperatures of the two peaks are higher by about 100 K than those of the Ar-ion sputtered surface. It may be due to a contamination of carbon on the surface. However, the shape of two spectra and the difference between the desorption peaks of the α-state and the

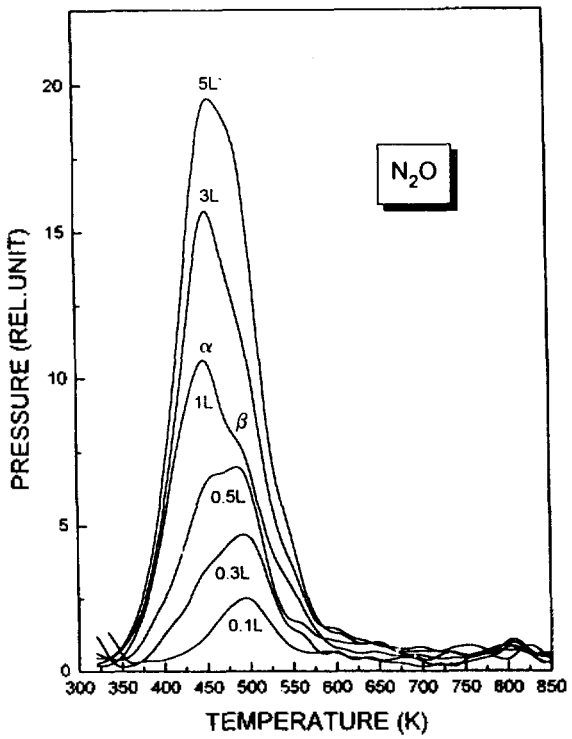

Figure 5. Thermal desorption spectra of N_2O formed with different exposures of NO.

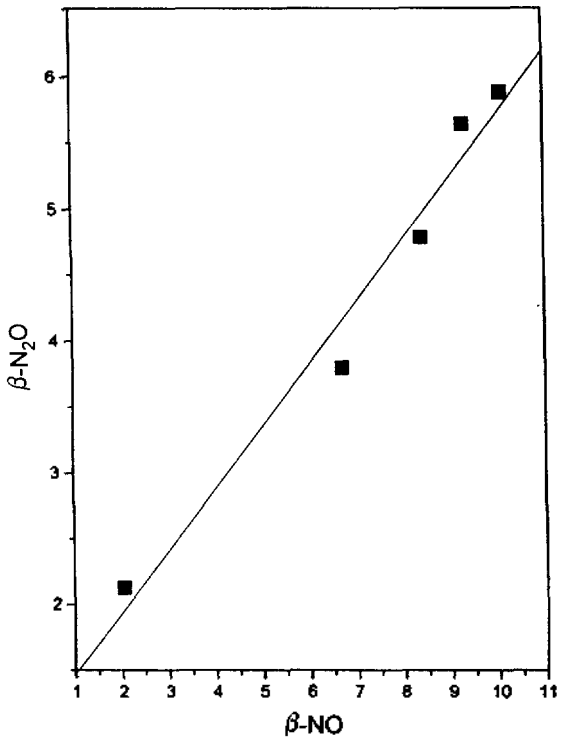

Figure 6. Relation of the amount of β-N_2O to β-NO.

β-state are similar to those obtained from the Ar-ion sputtered surface. These results suggest that the peaks are attributed to the terrace and the step of the surface, respectively.

Above the exposure of 0.3 L NO the peak for the α-state shifts slowly from 525 K to 530 K and the peak for the β-state is no longer observed. As shown in Figure 3, the amount of the desorbed N_2 from the β-state is about 25% of total amount of desorbed N_2. Since the population of β-N_2 is much smaller than that of α-N_2, the peak of N_2 for the β-state could be buried in the large band of α-N_2 at the high coverages. The desorption activation energies of N_2 from the α-state and the β-states are estimated to be 31.8 and 36.6 kcal/mol, respectively. The desorption of N_2 from NO adsorbed on Pt surfaces has been observed only with appearance of the strong binding state similar to the β-state,[7,9,22,24] indicating that NO in the strong binding state plays an important role on the dissociation of NO.

In addition to N_2 and NO we observed small desorption peaks at mass of 44. We interpreted them as the formation of N_2O in a reaction of adsorbed species on the Pt surface. Figure 5 shows a set of TDS of N_2O taken simultaneously with those of NO and N_2 with different exposures of NO. At 0.1 L NO exposure only one peak is observed at 480 K while at the exposure of 0.3 L a second peak at 450 K begins to appear as a shoulder of the first peak and grows gradually with increasing NO exposure. These peaks are designated as α and β, respectively. Since the appearance of two peaks implies a reaction of the adsorbed species at different states, it seems reasonable that the α peak is associated with the formation of N_2O from the species adsorbed on the (111) terrace sites and the β peak from those adsorbed on the step sites. The desorption temperatures of these peak are constant with increasing coverage, which is a characteristic of a first-order desorption kinetics. Assuming the first-order kinetics, the activation energies for α and β-N_2O are estimated to be 27 and 29 kcal/mol, respectively.

As shown in Figure 3, while the α-N_2O peak increases with NO exposure, the β-N_2O peak remains nearly constant above 0.5 L NO. But the α-N_2O and the β-N_2O peaks increase in parallel with the N_2 and the NO peaks in each states. This suggests the formation of N_2O is closely related to N_2 and NO adsorbed in the α-state and the β-state, respectively. Figure 6 shows a linear relation of the amount of β-N_2O to β-NO. This indicates that a fraction of β-NO converts to β-N_2O while heating the sample.

We have so far observed two characteristic peaks for the desorbed NO, N_2 and N_2O. Hence, in order to get information for the relationship between their desorbed species effects of temperature on the adsorption of NO were investigated. Figure 7 shows the desorption spectra of NO, N_2 and N_2O after adsorption of 5 L NO at different adsorption temperatures. Figure 8 shows quantitatively a relationship between the amount of desorbed species as a function of adsorption temperature. The α-peak of NO decreases gradually with adsorption temperature, while the β-peak of NO remains constant. The decrease of the α-peak is attributed that α-NO pre-desorbs above 315 K. The α-peak of N_2O also decreases gradually with adsorption temperature even though α-N_2O does not desorb in the range of the adsorption temperature. As a result, with increasing adsorption temperature both the amounts of desorbed α-NO and α-N_2O decrease even though their slopes are not same. This supports that the formation of α-N_2O is closely related to the population of α-NO in agreement with the results for NO adsorption at room temperature. That is, $\alpha\text{-NO}+\alpha\text{-N}_{ad}\rightarrow\alpha\text{-N}_2O$. If so, the difference

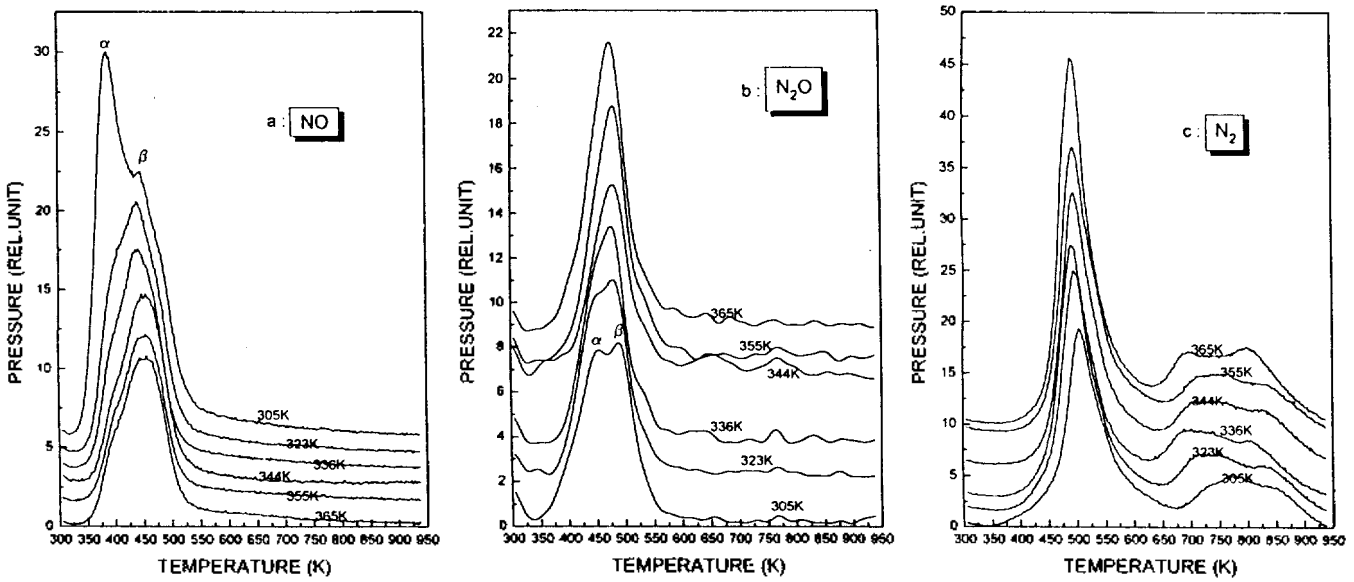

Figure 7. Thermal desorption spectra of NO (a), N_2O (b), N_2 (c).

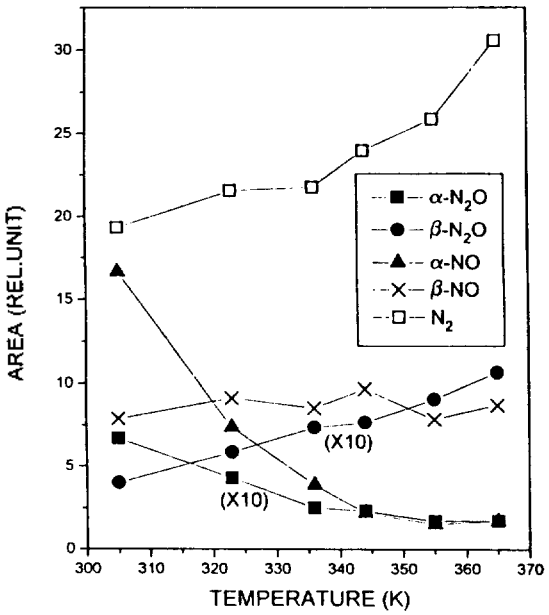

Figure 8. Adsorption temperature dependence of the relative amount of the desorbed species after NO adsorption of 5 L exposure at different temperatures.

of their slopes implies that a fraction of conversion of α-NO to α-N_2O increases with increasing adsorption temperature. On the other hand, with increasing adsorption temperature the β-peak of N_2O increases rather slowly in parallel with increase in N_2, suggesting that the atomic nitrogen in the terrace (the α-state) contributes to the formation of β-N_2O. Figure 8 shows that the peak of N_2 also increases with adsorption temperature. Assuming that atomic nitrogens formed by dissociation of NO recombine to form molecular nitrogen, the increase in desorbed nitrogen with adsorption temperature implies that dissociation of NO is an activation process.

Assuming that the appearance of N_2 is a direct measure of the dissociation of NO, we can write the rate of NO dissociation,

$$\frac{d\theta_N}{dt} = A \exp\left(-\frac{E_a}{RT}\right) P_{NO} = k P_{NO}$$

where θ_N is the amount of atomic nitrogen on the surface, P_{NO} is the pressure of NO in the gas state, E_a is the activation energy of NO dissociation on the surface, A is a pre-exponential factor and k is a rate constant. Since one Langmuir is a unit of gas exposure of 1×10^{-6} torr·sec, the amount of N_2 desorbed at different temperatures is equal to the amount of dissociation of NO for 1 sec under the pressure of 1×10^{-6} torr. Therefore, the activation energy of NO dissociation can be obtained from Arrhenius plot of the amount of N_2 at many temperatures (Figure 9) and estimated to be about 2 kcal/mol.

Discussion

The results of this study are in good agreement with previous ones for the defect or stepped surfaces.[14,17,19] Comparing the shape and the behavior of desorption spectra of NO and N_2 with ones in ref. 19, one finds that the surface of sample used in this experiment has a structure similar to Pt(211).

The desorption spectra of NO show two characteristic peaks at 370 and 470 K designated as α and β, respectively. These peaks are consistent with our previous study for the Ar-ion sputtered Pt(111) surface.[17] The Ar-ion sputtering creates the defect sites on Pt(111) surface, and produces the second peak at 450 K in addition to the peak at 380 K for clean Pt(111) surface. Therefore, we assign these two peaks at 370 and 470 K to the flat surface and to the step sites, respectively. According to the results from vibrational spectroscopy for NO adsorption on a well-annealed surface at low coverage,[13,15] the adsorbed NO was characterized by a band near 1500 cm^{-1}, which corresponds to molecularly adsorbed species at the two-fold bridge sites. On the other hand, the peak near 1700 cm^{-1} observed at high coverage

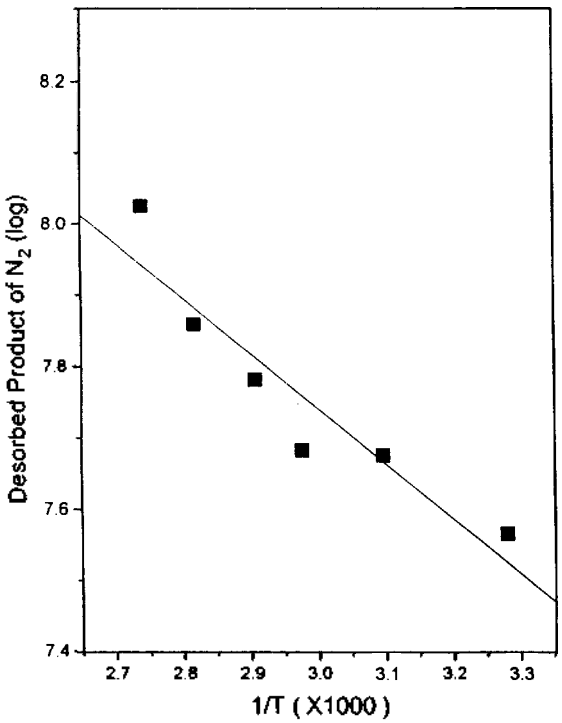

Figure 9. Arrhenius plot of the amount of N_2 formed from decomposition of NO on the stepped Pt(111) surface.

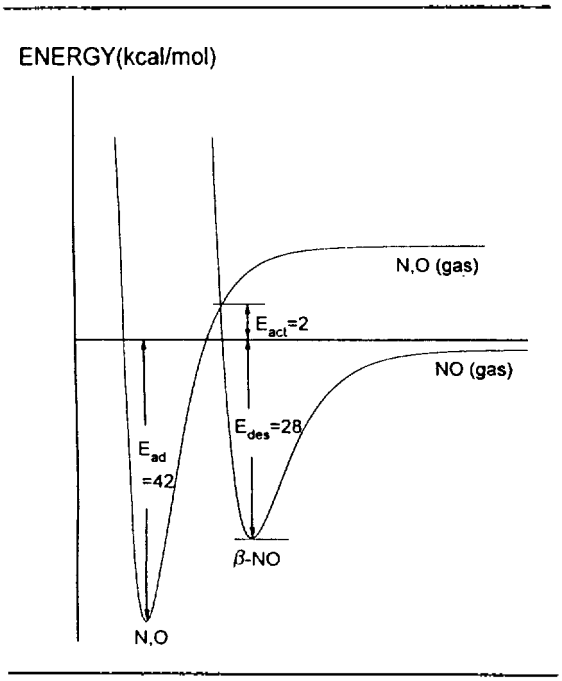

Figure 10. Potential energy diagram for the NO dissociation.

was interpreted as on-top bound NO at the terrace sites.

In a more recent study for the interaction of NO with different defect concentrations using IR spectroscopy,[16] two characteristic peaks in the range of 1609-1634 cm^{-1} and in the range of 1820-1840 cm^{-1} were observed in addition to the two peaks due to adsorption of NO on the terrace as mentioned above. Based on comparison of these two peaks with the results for the flat surface, the low frequency peak (1609-1634 cm^{-1}) was assigned to a terminal bent species adsorbed at the defect sites and the higher frequency peak (1820-1840 cm^{-1}) to the species of a linear configuration. Thus, the vibrational spectroscopic data suggest that NO adsorbs molecularly in both the α-state and the β-state and that the α-state can be characterized by the NO species adsorbed at the two-fold bridge sites and at the on-top sites. They also indicate that the β-state can be characterized by the Pt-N-O species with a bent geometry and a linear species.

Studies of metal nitrosyl complex[25,26] concludes that the binding of NO to metals occurs generally through the nitrogen atom which donates its lone pair electrons to the metal *d*-orbitals to form a σ-bond. In addition, a backbonding of metallic *d* electrons into the lowest π^* orbital contributes to the metal-NO bond. According to this general scheme, a lower frequency of NO stretching vibration implies a stronger Pt-NO bond. Therefore, only the higher frequency peak of the two peaks near 1500 cm^{-1} (two-fold site species) and 1700 cm^{-1} (on-top species) that are assigned to NO species adsorbed on the terrace is reasonably compared to the lower frequency peak of the two peaks near 1620 cm^{-1} and 1830 cm^{-1} for NO at the step site. This is explanable if the on-top species on terrace has a higher stretching frequency of N-O than the bent species at the step sites and hence the former has a lower binding energy than the latter. But the two fold species with lower frequency on the terrace and the linear species with higher frequency at the step sites in the observed spectra[15,16] are not explanable with the results of TDS.

Gumhalte *et al.*[27] have recently investigated theoretically the effect of step sites on the adsorption of CO. The strong potential difference between the terrace and the step gives rise to a strong localized electric field parallel to the surface plane and hence a lateral surface Stark effect acts on the adsorbed molecules near the step. This lateral surface Stark effect will lead to a shifting and splitting of the π^*-derived resonance of adsorbed CO molecules and to an increased electronic backdonation. Since NO has similar electronic structures, the lateral surface Stark effect explains the appearance of the strong bound state of NO at the step sites.

Another important observation in Figure 3 is that more atomic nitrogen is presented than expected from the ratio of the number of step sites to the number of terrace sites. This suggests that the step provides only a precursor state from which a large fraction of atomic nitrogen diffuses immediately into the terrace. If so, we expect that the desorption of N_2 comes from the two states, the terrace and the step. In fact, Figure 4 shows the existence of the two states : at low coverages the peak for the β-state can be identified and at high coverages the α-state peak is dominant.

To be sum, the bent species at the step characterized by near 1600 cm^{-1} is a precursor, and the dissociated atomic nitrogen diffuses into the terrace. Thus, the step plays a role of forming a favorable species for the dissociation of NO and is available for forming the next precursor after the removal of N by the diffusion. This implies the rate of dissociation of NO from the precursor state at the step is dependent on the diffusion of the dissociated atomic N into the terrace. As we can see in Figure 8, the rate of

the dissociated nitrogen from NO increases with adsorption temperature at a fixed amount of exposure, even though the amount of desorbed NO from the α-state decreases and that from the β-state remains constant. This emphasizes the importance of the diffusion of the dissociated nitrogen atom at the step, because the unoccupancy of NO in the α-state probably facilitate the dissociated nitrogen to diffuse into terrace. Perhaps, the diffusion is responsible for the low activation energy of the NO dissociation, 2 kcal/mol, which is close to 10% of half the desorption enengy of N_2. Here, the activation energy of surface diffusion is assumed less than 10% of the desorption energy of the surface species, and the desorption energy of atomic N is half the desorption energy of N_2.

A final important observation in Figures. 1 and 5 is the appearance of N_2O produced in the second reaction of adsorbed species on the surface during the desorption process. This formation of N_2O has been paid little attention because its amount is below 10% of other desorption products. This species was observed in the spectra only when N_2, formed from the dissociation of NO, appears in the corresponding spectra. It implies that NO and N on the surface combine to produce N_2O. This excludes another possible mechanism for the formation of N_2O by combination of two NO species on the surface ($NO+NO\rightarrow N_2O$). The decrease in α-N_2O and α-NO with increasing adsorption temperature in Figure 8 indicates that α-N_2O is produced in the reaction of N and NO on the terrace.

The reason for the different slopes of decrease in the amount of α-N_2O and α-NO is because the rate of forming N_2O is limited by the amount of N at low adsorption temperature and by the amount of NO at high adsorption temperature. While the amount of β-NO remains constant at all adsorption temperatures, slow increase of β-N_2O with adsorption temperature suggests that the diffusion of α-N from the terrace to the step contributes to the formations of β-N_2O; $\alpha\text{-N}\rightarrow\beta\text{-N}$ (diffusion process), $\beta\text{-NO}+\beta\text{-N}\rightarrow\beta\text{-N}_2\text{O}$. Thus, we conclude that the desorbed N_2O is produced in the surface reaction of the adsorbed NO and the atomic N and that the observed two peaks originate from NO and N adsorbed at the different sites of the α-state and the β-state.

Acknowledgment. The present studies were in part supported by the Basic Science Research Institute Program, Ministry of Education, Korea, 1994 (BSRI-94-6401) and in part by the Korea Science and Engineering Foundation (92-25-00-06).

Reference

1. Lambert, R. M.; Bridge, M. E. In *The Chemical Physics of Solid Surface and Heterogeneous Catalysis*; King, D. A.; Woodruff, D. P., Eds.; Elsevier Scientific: New York, 1984; Vol. 3, p 59.
2. Campbell, C. T.; Ertl, G.; Kuppers, H.; Segner, J. *Surf. Sci.* **1981**, *107*, 207.
3. Kiskinova, M.; Szabo, A.; Yates, J. T. *Surf. Sci.* **1988**, *205*, 215.
4. Egehoff, Jr. W. F. In *The Chemical Physics of Solid Surface and Heterogeneous Catalysis*; King, D. A.; Woodruff, D. P., Eds.; Elsevier Scientific: New York, 1984; Vol. 4; p 424.
5. Lambert, R. M.; Comrie, C. M. *Surf. Sci.* **1974**, *46*, 61.
6. Comrie, C. M.; Weinberg, W. H.; Lambert, R. M. *Surf. Sci.* **1976**, *57*, 619.
7. Gorte, R. J.; Schmidt, L. D.; Gland, J. L. *Surf. Sci.* **1981**, *109*, 367.
8. Gland, J. *Surf. Sci.* **1978**, *71*, 327.
9. Campbell, C. T.; Ertl, G.; Segner, J. *Surf. Sci.* **1982**, *115*, 309.
10. Kiskinova, M.; Pirug, G.; Bonzel, H. P. *Surf. Sci.* **1984**, *140*, 1; **1984**, *136*, 285.
11. Pirug, G.; Bonzel, H. P. *J. Catal.* **1978**, *53*, 96.
12. Bonzel, H. P.; Pirug, G. *Surf. Sci.* **1977**, *62*, 45.
13. Hayden, B. E. *Surf. Sci.* **1983**, *131*, 419.
14. Pirug, G.; Bonzel, H. P. *J. Catal.* **1977**, *50*, 64.
15. Gland, J.; Sexton, B. E. *Surf. Sci.* **1980**, *94*, 355.
16. Agrawal, V. K.; Trenary, M. *Surf. Sci.* **1991**, *259*, 116.
17. Boo, J. H.; Kang, Y. C.; Song, M. C.; Park, C. Y.; Kwak, H. T.; Lee, S. B. *J. Korean Vac. Soc.* **1993**, *2*, 404.
18. Boo, J. H. Ph.D. Dissertation, Sung Kyun Kwan University, 1992.
19. Gohndrone, J. M.; Masel, R. I. *Surf. Sci.* **1989**, *209*, 44.
20. Redhead, P. A. *Vacuum* **1962**, *12*, 203.
21. Burgess, Jr. D.; Cavanagh, R. R.; King, D. S. *Surf. Sci.* **1989**, *214*, 358.
22. Wickham, D. T.; Banse, B. A.; Koal, B. E. *Surf. Sci.* **1989**, *223*, 82.
23. Banhholzer, W. F.; Gohndrone, J. M.; Hatziks, G. H.; Masel, R. I.; Park, Y. O.; Stolt, K. *J. Vacuum Sci. Tecnol.* **1985**, *A3*, 1559.
24. Banhholzer, W. F.; Masel, R. I. *J. Catal.* **1984**, *85*, 127.
25. Cotton, F. A.; Wilkinson, G. In *Advanced Inorganic Chemistry*; 5th Ed., Wiley: New York, 1988; p 336.
26. Richtor-Addo, G. B.; Legzdins, P. *Metal Nitrosyls*; Oxford Press: New York, 1992.
27. Gumhalter, B.; Hermann, K.; Wandelt, K. *Vacuum* **1990**, *41*, 192.